COst REduction and increase performance of floating WIND technology

(COREWIND)

H2020-LC-SC3-2018-RES-TwoStages / Grant Agreement 815083

D1.1 Definition of the 15 MW Reference Wind Turbine

Henrik Bredmose (ed), Jennifer Rinker, Witold Skrzypinski, Frederik Zahle, Fangzhong Meng, Katherine Dykes (DTU)

Evan Gaertner, Garrett Barter, Pietro Bertolotti, Latha Sethuraman and Matt Shields (NREL)

"This project has received funding from the European Union's Horizon 2020 research and innovation programme under grant agreement No 815083".

Project acronym	COREWIND
Grant Agreement Nº	815083
Project title	COst REduction and increase performance of floating WIND technology
Website	*(under definition)*

Deliverable	D1.1
Title of deliverable	Definition of the 15MW Reference Wind Turbine
Work package	WP1
Dissemination level	Public
Document version	V1
Delivery Date	31/10/2020
Authors (Main Beneficiary)	DTU
Other Contributors	NREL

Version	Date	Author	Organisation	Comments
1	23 Oct 2019	H. Bredmose et al	DTU	Advanced draft
2	31 Oct 2019	H. Bredmose et al	DTU	Final

ABBREVIATION LIST

BECAS	BEam Cross section Analysis Software (DTU)
BTC	Bend-Twist Coupling
DLB	Design Load Basis
DTU	Technical University of Denmark
FAST	Fast Aeroelastic Simulation Tool (NREL)
HAWC2	Horizontal Axis Windturbine Code version 2 (DTU)
HAWCStab2	Steady state version of HAWC2 for stability analysis
HAWTOpt	Horizontal Axis Wind Turbine Optimization tool (DTU)
NREL	National Renewable Energy Laboratory
PID	Proportional-Integral-Derivative (control)
RNA	Rotor-Nacelle Assembly
RWT	Reference Wind Turbine
TSR	Tip-Speed Ratio

EXECUTIVE SUMMARY

A preview of the IEA 15MW reference wind turbine.

The present deliverable defines a 15 MW reference wind turbine, implemented in the aero-elastic HAWC2 model. The turbine feeds into the further activities in WP1 and the rest of COREWIND, and will form the basis for the floater designs of COBRA and UPC.

The turbine is a preview of the IEA 15 MW Reference Wind Turbine, which has been defined by NREL. The turbine has been implemented in DTUs aero-elastic models HAWOpt, HAWCStab2 and HAWC2. This process has been a driver for strong interaction between the NREL and DTU teams and stimulated iterations on the design.

The present deliverable provides a preview of the IEA design, which will be released by the end of 2019. It further provides the HAWC2 implementation of the turbine, including a tuned controller and a provisional bend-twist blade design, intended for load reduction around rated wind speed.

The key features of the turbine are the 15 MW rated power, a rotor diameter of 240m, direct drive generator and (for the HAWC2 version) a provisional bend-twist coupled design.

Links to the IEA and HAWC2 repositories are given in the report.

Contents

1 A preview of the IEA 15 MW reference wind turbine

The present report provides a preview of the IEA 15MW reference wind turbine, designed by NREL and with further interaction and HAWC2 implementation by DTU. The official and fully public release of the IEA wind turbine will take place by the end of 2019.

1.1 The importance of reference wind turbines

Reference wind turbines are important for the wind energy community. They serve as realistic benchmark models, defined with publically available design parameters. They allow transparent research and development projects, even for actors not deeply acquainted with wind turbine technology or design.

The history of reference wind turbines is largely dominated by the NREL 5 MW turbine Jonkman et al. (2009) and the DTU 10MW turbine Bak et al. (2013). These turbines have been supplemented by other turbines, such as an 8 MW turbine in the EU FP7 project LEANWIND Desmond et al. (2016), the 3.4 MW land-based and 10 MW offshore IEA task 37 reference turbines Bortolotti et al. (2019), and a conceptual study of a 20 MW turbine in the INNWIND project INNWIND.EU (2017). The tradition within reference wind turbines has been to release a realistic, but often not fully optimized design, which can next be updated and improved by the active wind energy community.

The size of wind turbines is still increasing. For bottom fixed offshore wind energy, the average turbine size for European deployment in 2018 was 6.8 MW (WindEurope (2019)), and GE will launch its 12 MW Haliade-X offshore turbine to the market in 2021.

Thus for continued development of e.g. foundation design, wind farm control and logistic studies, a reference wind turbine above 10 MW is needed. This is the motivation for the IEA 15 MW reference wind turbine. The turbine is in the present report provided in its land-based version, with a tower rigidly clamped to the ground. The official IEA design will include a monopile foundation too. Floater designs for the turbine will follow after the first release.

1.2 Key features

The turbine parameters are described in Section 2. The key features are

- 15 MW rated power
- 10.77 m/s rated wind speed

- 240 m rotor diameter
- 150 m hub height
- Direct drive generator
- A provisional bend-twist coupled design in the HAWC2 version, intended to reduce the loads around rated wind speed.

1.3 People and contributors

The turbine has been defined by NREL (National Renewable Energy Laboratory) within the IEA task 37. The team consists of Evan Gaertner, Garrett Barter, Pietro Bertolotti, Latha Sethuraman and Matt Shields.

Next, under the H2020 COREWIND project, the preliminary design have been provided to DTU. Here, the design has been implemented into DTU's HAWTOpt2, HAWCStab2 and HAWC2 tools. This process has stimulated iterations on the design, such that the resulting turbine has now been checked at both NREL and DTU, and is available at both the FAST and HAWC2 platforms. The DTU team consists of Jennifer Rinker, Witold Skrzypiński, Frederik Zahle, Fanzhong Meng, Katherine Dykes and Henrik Bredmose.

The official release of the IEA 15MW reference wind turbine will take place by the end of 2019.

1.4 Access to the model

The turbine and models in FAST and HAWC2 is available at the following IEA Github site

`https://github.com/IEAWindTask37/IEA-15-240-RWT`

Here, also updates of the turbine and additional foundation and floater models will be posted.

2 Overall turbine parameters

The overall parameters for the turbine are stated in Table 1. The table also shows the data for the DTU 10 MW reference wind turbine for comparison.

Parameter	DTU 10MW turbine	IEA 15MW turbine
Turbine Class	IEC Class 1B	
Specific rating	401 W/m^2	332 W/m^2
Rotor orientation	Upwind	Upwind
Control	Variable speed, collective pitch	Variable speed, collective pitch
Cut-in wind speed	4 m/s	3 m/s
Rated wind speed	11.4 m/s	10.56 m/s
Cut-out wind speed	25 m/s	25 m/s
Rotor diameter	178.3 m	240 m
Hub height	119 m	150 m
Hub diameter	5.6 m	6 m
Drive train	Medium speed. Multiple-stage gearbox	Low speed. Direct drive
Design tip speed ratio	7.5	9.0
Minium rotor speed	6.0 rpm	4.6 rpm
Maximum rotor speed	9.6 rpm	7.6 rpm
Maximum tip speed	90 m/s	95 m/s
Gear box ratio	50	—
Shaft tilt angle	5.0 deg	6 deg
Rotor pre-cone angle	-2.5 deg	-4 deg
Blade pre-bend	3.332 m	4 m
Blade mass	41 t	65.7 t
RNA mass	674 t	1446 t
Tower mass	628 t	1211 t
Tower diameter at base	8.0 m	10 m

Table 1: Overall parameters for the IEA 15 MW turbine, compared to the DTU 10 MW turbine.

3 Blade Properties

The blade aerostructural properties were computed based on the blade design provided by NREL[1].

3.1 Blade aerodynamic properties

Figure 1 shows the aerodynamic characteristics of the airfoils used on the blade. The airfoil characteristics are based on Xfoil computations, assuming free transition, i.e. clean surface conditions.

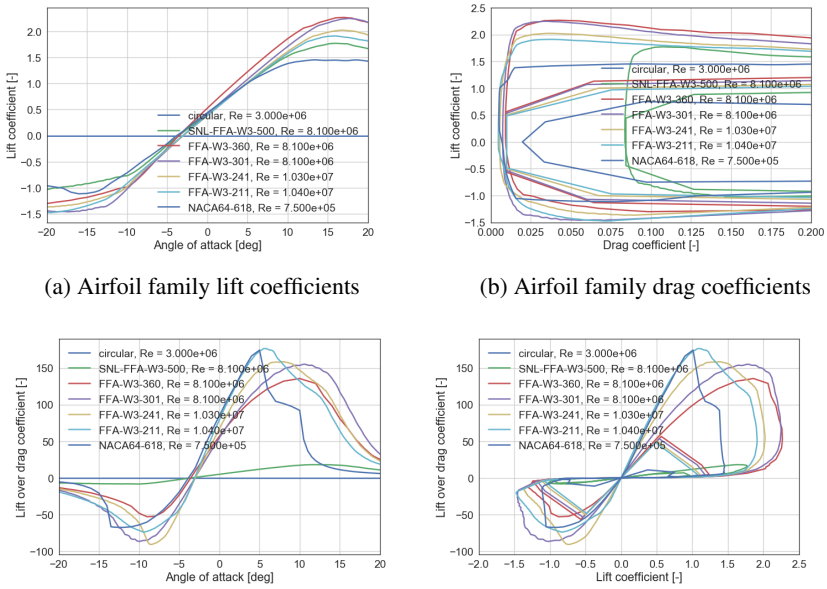

(a) Airfoil family lift coefficients

(b) Airfoil family drag coefficients

(c) Airfoil family lift-to-drag coefficients vs angle of attack

(d) Airfoil family lift-to-drag coefficients vs lift coefficient

Figure 1: Aerodynamic performance coefficients for the airfoils used on the blade.

The blade planform is plotted in Figure 2.

[1]https://github.com/IEAWindTask37/IEA-15-240-RWT, commit-sha: b372f1e81a74c712b563db82827cc3c9b2ad87df

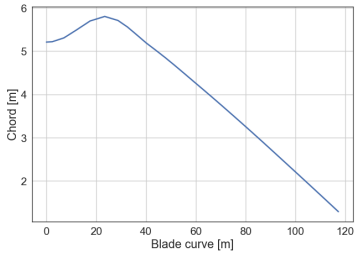

(a) Chord length vs blade-curve position

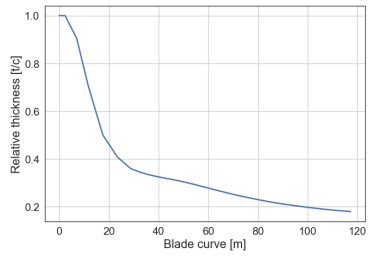

(b) Relative thickness vs blade-curve position

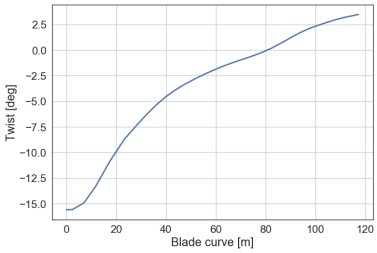

(c) Twist vs blade-curve position

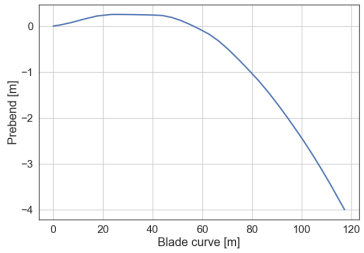

(d) Prebend vs blade-curve position

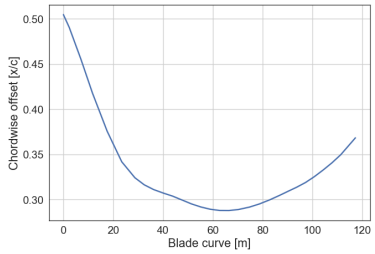

(e) Chordwise offset vs blade-curve position

Figure 2: Blade planform

3.2 Blade structural properties

The internal structural layout is illustrated in Figure 3, showing the lofted blade viewed from the tip towards the root, with the location of the trailing edge reinforcement, spar cap and leading edge reinforcement regions indicated with red circles along the span.

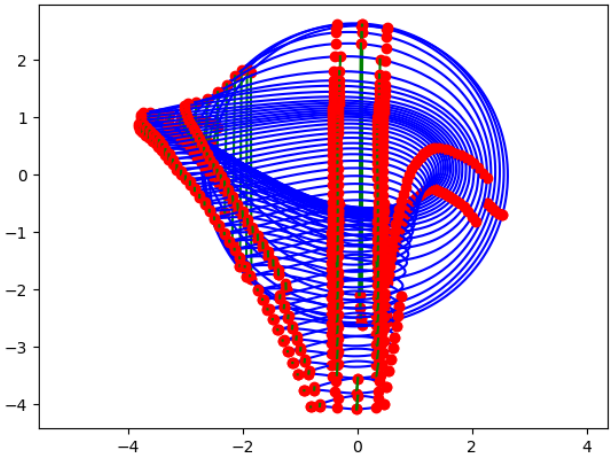

Figure 3: Lofted blade seen from the tip. The trailing edge reinforcement, spar cap and leading edge reinforcement regions are indicated with red circles along the span

The material layup is plotted in Figure 4, showing the key regions of the blade.

The blade beam structural properties were computed using BECAS Blasques (2012); Blasques and Stolpe (2012) based on the geometrically resolved lofted blade structure computed using HAWTOpt2 Zahle, Tibaldi, Verelst, et al. (2015); Zahle, Tibaldi, Pavese, et al. (2016). Figure 5 shows the cross-sectional mesh generated using the mesh generator Shell expander, a companion utility to BECAS.

BECAS computed the fully populated stiffness matrix for each cross-section along the blade, which can be read directly into HAWC2. Figure 6 shows the resulting blade beam structural properties.

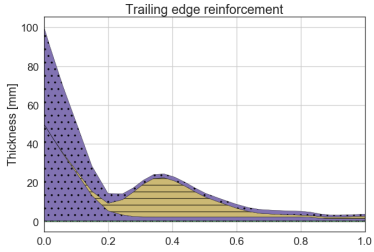

(a) Thickness of layers in the trailing-edge-reinforcement region vs normalized blade-curve position

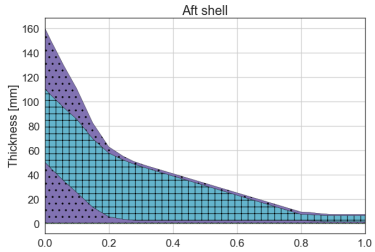

(b) Thickness of layers in the aft-shell region vs normalized blade-curve position

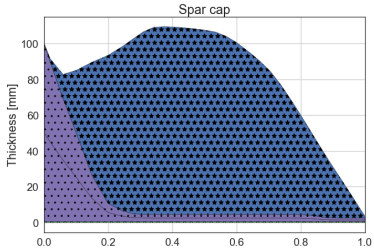

(c) Thickness of layers in the spar-cap region vs normalized blade-curve position

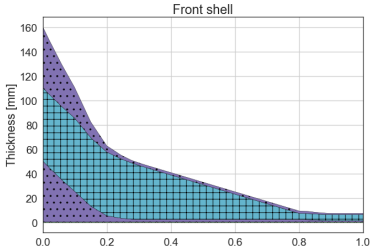

(d) Thickness of layers in the front-shell region vs normalized blade-curve position

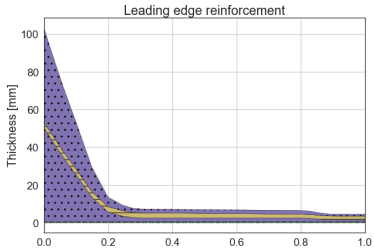

(e) Thickness of layers in the leading-edge-reinforcement region vs normalized blade-curve position

Figure 4: Blade layup

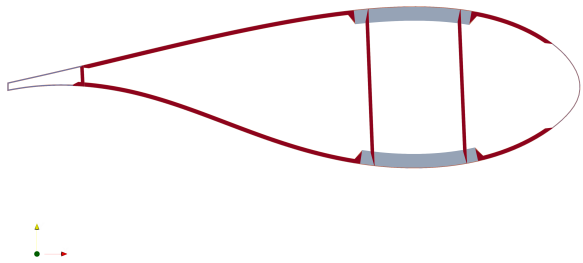

Figure 5: Cross-sectional mesh for r/R=0.50 used to compute the sectional beam properties.

3.2.1 Blade damping values

The blade damping was modeled using HAWC2's anisotropic damping model, which is appropriate for bodies that utilize fully populated matrices. The mass-proportional terms were set to zero to avoid any potential numerical issues. The stiffness-proportional terms were tuned such that the damping on the first flapwise and edgewise modes were near 3% and the damping on the first torsional mode was as low as possible. The torsional mode was not able to achieve lower damping because the damping matrix was no longer positive definite if η_t^s was reduced too much. The resulting damping values are given in Table 2.

Table 2: HAWC2 stiffness-proportional damping values for blade

η_x^s	η_y^s	η_z^s
3.23e-3	2.85e-3	1.0e-4
Flap. log dec	Edge. log dec	Tors. log dec
3.00%	3.00%	6.08%

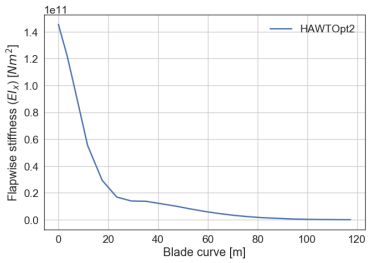

(a) Flapwise stiffness vs blade-curve position

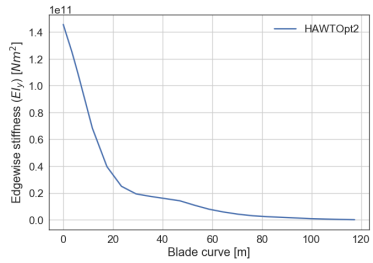

(b) Edgewise stiffness vs blade-curve position

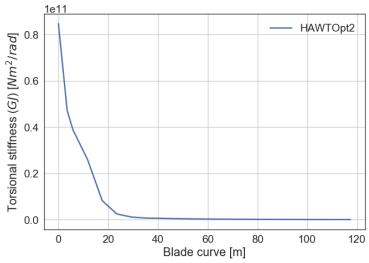

(c) Torsional stiffness vs blade-curve position

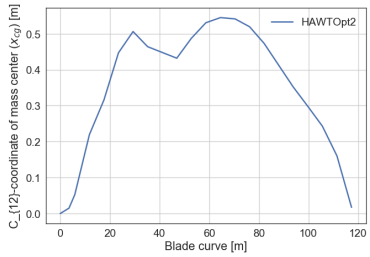

(d) C(12) coordinate of mass center vs blade-curve position

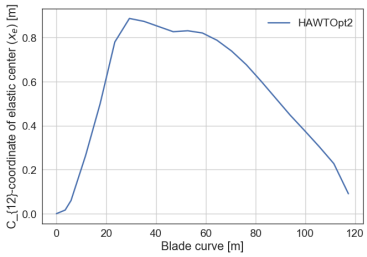

(e) C(12) coordinate of elastic center vs blade-curve position

Figure 6: Blade beam structural properties computed using BECAS Blasques (2012); Blasques and Stolpe (2012).

4 Rotor steady state performance

The steady state performance of the rotor was modelled in HAWCStab2. Here the turbine performance at constant wind speed is modelled with the blade element momentum method, including control. The steady-state computation eliminates the need for time-integration of the full equations of motion. Yet, the solution is fully consistent with a full time domain simulation.

Figure 7 shows the rotor steady state power curve, thrust, power and thrust coefficients as function of wind speed, computed using HAWCStab2. The steady thrust has a maximum value close to 2100 kN and a maximum power coefficient of $C_P \simeq 0.48$.

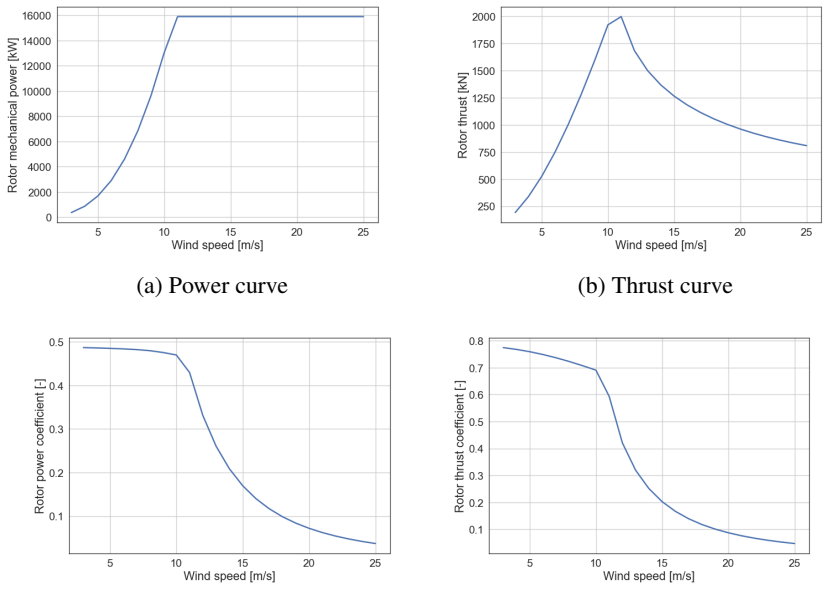

(a) Power curve

(b) Thrust curve

(c) Rotor global power coefficient

(d) Rotor global thrust coefficient

Figure 7: Rotor steady state aerodynamic performance computed with HAWCStab2

Further analysis of the blade performance is shown in Figures 8 and 9. Here, the distributed aerodynamic characteristics of the blade computed over a range of wind speeds below rated wind speed. It can be seen that the blade load decreases towards the tip. More insight is provided in plot (c) of the local thrust coefficient. Here the

maximum value is achieved around a radius of $r = 30$ m, with strong reduction visible from $r = 100$ m.

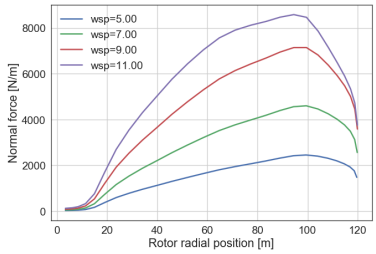

(a) Normal force on the blade vs rotor radial position

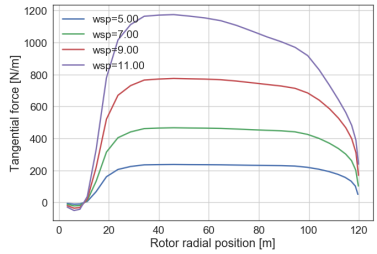

(b) Tangential force on the blade vs rotor radial position

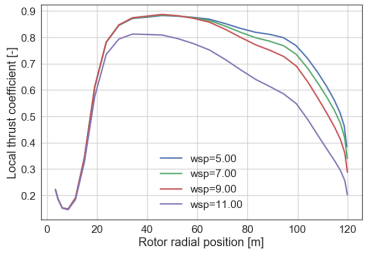

(c) Local thrust coefficient vs rotor radial position

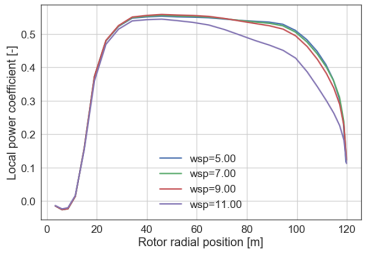

(d) Local power coefficient vs rotor radial position

Figure 8: Blade steady state aerodynamic performance computed with HAWCStab2

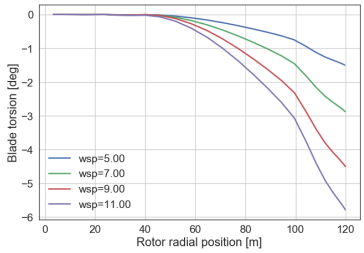

(a) Blade torsion vs rotor radial position

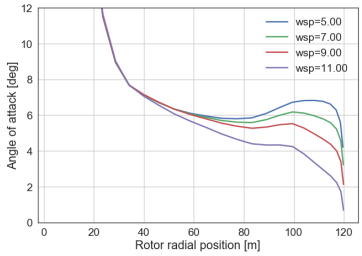

(b) Angle of attack vs rotor radial position

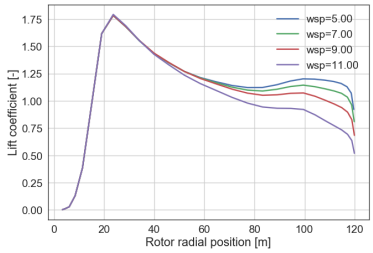

(c) Lift coefficient vs rotor radial position

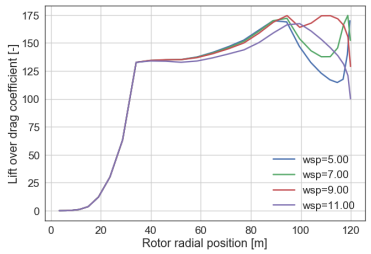

(d) Lift-over-drag coefficient vs rotor radial position

Figure 9: Blade steady state aerodynamic performance computed with HAWCStab2

5 Tower properties

The tabulated values for the wall thickness and outer diameter are given in Appendix A. These values were determined by NREL using WISDEM's TowerSE code.

The tower is modelled as an isotropic steel tube. The thickness and outer diameter shown in Figure 10. The material properties are stated in Table 3.

Table 3: Material properties for tower

Parameter	Symbol	Value
Young's modulus	E	2.00E11 Pa
Shear modulue	G	7.93E10 Pa
Density	ρ	7.85E3 kg/m^3

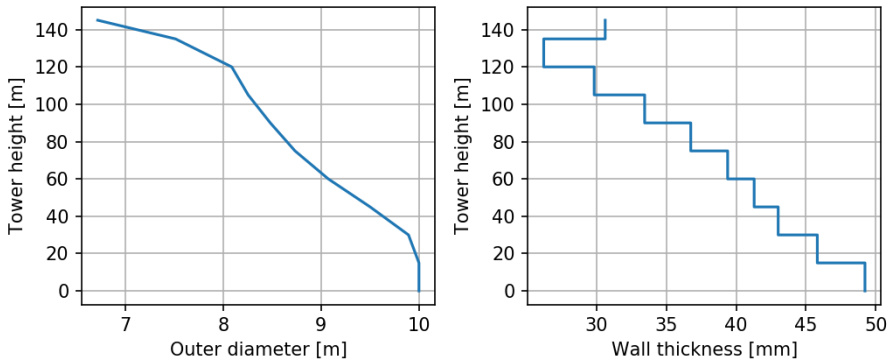

Figure 10: Outer diameter and wall thickness for tower

The tower is modelled in HAWC2 using a Timoshenko beam with 10 elements. The edges of the elements are given in Table 4.

The HAWC2 structural parameters for the Timoshenko beam were determined using the equations given in Appendix B. These structural parameters were compared to BModes output provided by NREL using the following relationships:

- Mass density is equal to m
- Flapwise inertia is equal to $m\,r_{ix}^2$

Table 4: Element edges in `c2_def` block

Node index	Node station
1	0
2	15
3	30
4	45
5	60
6	75
7	90
8	105
9	120
10	135
11	145

- Edgewise inertia is equal to $m r_{iy}^2$
- Flapwise stiffness is equal to EI_x
- Edgewise stiffness is equal to EI_y
- Torsional stiffness is equal to GK
- Axial stiffness is equal to EA

The comparison with the BModes output is given in Figure 11. The two methods match perfectly.

The damping for the tower is stiffness-proportional only, to avoid numerical issues with HAWC2's mass-proportional damping. The stiffness-proportional factors for the x, y and z directions (respectively, K_x, K_y and K_z, corresponding to fore-aft, side-side and torsion) were determined by enforcing a 2% logarithmic decrement on the first fore-aft, side-side and torsional tower modes (modes 1, 2 and 7, respectively). The modal damping values for the tower were calculated using HAWC2's `body_eigenanalysis` option. The resulting damping values are given in Table 5.

Table 5: HAWC2 stiffness-proportional damping values for tower

K_x	K_y	K_z
1.671E-03	1.671E-03	1.357E-04

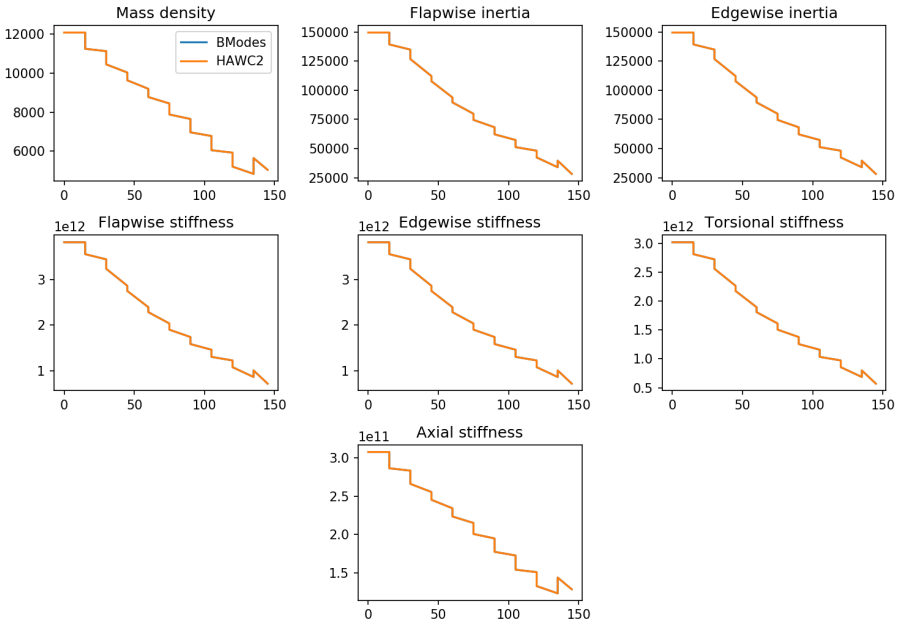

Figure 11: Comparison of HAWC2 and BModes tower parameters

6 Nacelle, drivetrain and hub

The geometry of the nacelle, drivetrain and hub were modelled in HAWC2 using four bodies:

- `Towertop`: A massless, stiff body connecting the towertop to the intersection of the yaw and shaft axes. This body yaws with the turbine.
- `Connector`: A massless, stiff body connecting the end of the towertop to the beginning of the shaft. This body is directed along the shaft rotational axis but does not rotate with the shaft.
- `Shaft`: A massless, torsional-deflection-only body connecting the end of the Connector to the hub apex.
- `Hub`: A massless, rigid body connecting the hub apex to the blade root. There are actually three identical Hub bodies, one for each blade.

The masses and the inertia of the nacelle, drivetrain and hub were modelled using four point masses/inertias:

1. A point mass located at `NacCM` (from FAST) representing the combined mass of everything above the tower except for the blades/hub (corresponds to `NacMass` in FAST);
2. A massless point inertia (I_x, I_y and I_z taken with respect to `NacCM`, above) located at `NacCM` representing the inertia of everything that yaws with the tower but does not spin with the shaft;
3. A massless point inertia (I_z; $I_x = 0$ and $I_y = 0$) at the beginning of the shaft representing the rotational inertia of the generator rotor/shaft;
4. A point mass/inertia (m and I_z; $I_x = 0$ and $I_y = 0$) at the end of the shaft representing the rotational inertia of the generator rotor and shaft (corresponds to `HubMass` and `HubIner` in FAST).

The masses and inertias for the hub and generator are given in Table 6.

The stiffness-proportional damping for the shaft was chosen to produce a 5% of critical modal damping for the free-free mode of the generator/rigid-rotor system. This value of 5% was chosen based on the value in the NREL 5 MW reference model. In

Table 6: Masses and inertias for nacelle and drivetrain

Parameter	Value
Downwind, vertical distance from towertop to nacelle CM	[-6.21, 3.45]
Nacelle mass	1,070,000 kg
Nacelle inertia around CM, tilt	7.558513e+06 kg-m^2
Nacelle inertia around CM, roll	7.900629e+06 kg-m^2
Nacelle inertia around CM, yaw	1.013478e+07 kg-m^2
Downwind, vertical distance from towertop to generator	[-6.23 m, 4.474 m]
Generator inertia around shaft	1.715930e+07 kg-m^2
Downwind, vertical distance from towertop to hub CM	[-11.32 m, 5.0 m]
Hub mass	1.788320e+05 kg
Hub inertia around shaft	7.277949e+05 kg-m^2

particular, it can be shown that the stiffness proportional term β should be chosen such that

$$\beta = 2\zeta\sqrt{\frac{I_{gen}I_{rot}}{K_{DT}(I_{gen}+I_{rot})}}, \tag{1}$$

where ζ is the desired modal damping, I_i is the generator or rotor inertia and K_{DT} is the equivalent stiffness of the drivetrain. For this turbine, the rigid rotor inertia is approximately 3.524605e+08 kg-m^2, calculated from the HAWC2 blade structural file while ignoring coning and prebend. This results in $\beta = 4.457544$e-04 for the torsional motion.

7 Stability analysis

A stability analysis was performed as an initial evaluation of the model performance. The analysis was performed using DTU Wind Energy's software HAWCStab2.

The evaluation of the model's stability featured several steps:

1. Determine the optimal operational setpoints (pitch and rotor speed) assuming no minimum rotor speed;
2. Perform an aeroelastic modal analysis and determine a minimum rotor speed such that the 3P frequency does not coincide with any tower modes;
3. Recalculate the optimal operational data with this minimum rotor speed;
4. Perform the aeroelastic modal analysis again with the minimum rotor speed enabled.

A minimum pitch angle of 0 degrees and an optimal TSR of 9.5 were assumed.

From the evaluation of the coincidence of the 3P frequency and the tower modes, a minimum rotor speed of 4.6 RPM was chosen. The operational data is given in Fig. 12, and the aeroelastic Campbell diagram is plotted in Fig. 13. Note the three regions of operation: at minimum rotor speed (3 m/s to 6 m/s), at optimal TSR (6 m/s to 10 m/s), and at rated rotor speed (10 m/s to 25 m/s). The aeroelastic natural frequencies and damping for a wind speed of 3 m/s are provided in Table 7.

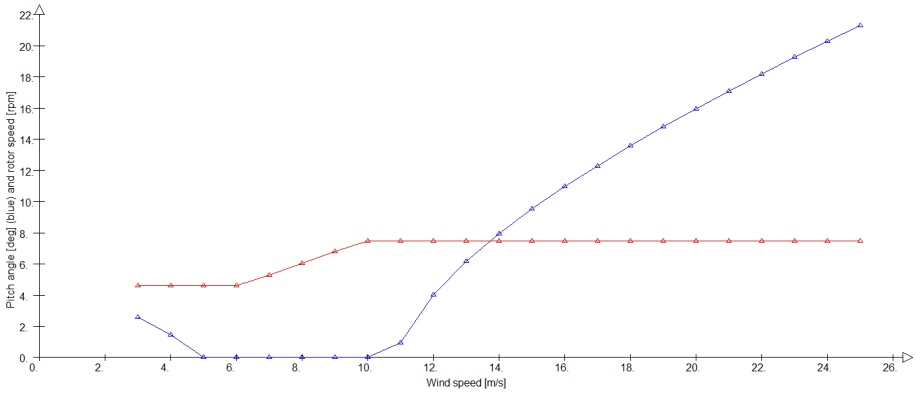

Figure 12: Optimal operational data determined using HAWCStab2 (red = rotor speed, blue = pitch angle)

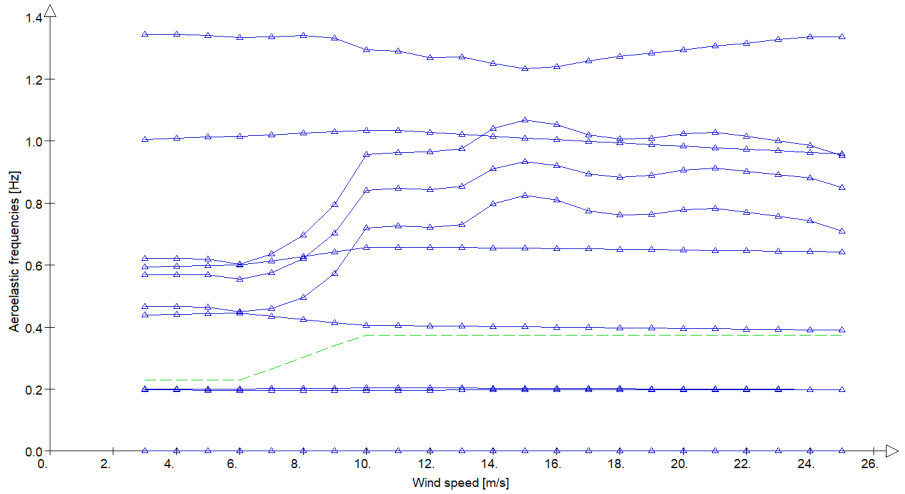

Figure 13: Aeroelastic Campbell diagram calculated using HAWCStab2. Green line indicates 3P.

Table 7: Aeroelastic mode shapes at 3 m/s

No.	Mode	Frequency (Hz)	Aeroelastic damping (% crit.)
1	1st Tower FA	0.20	4.87%
2	1st Tower SS	0.20	0.29%
3	1st Edge BW	0.44	1.97%
4	1st Flap BW	0.47	52.97%
5	1st Sym Flap	0.57	47.67%
6	1st Edge FW	0.59	2.06%
7	1st Flap FW	0.62	43.20%
8	1st DT	1.01	1.04%

8 Control

The wind turbine is regulated via the DTU Basic Controller Hansen and Henriksen (2013). For this wind turbine design, there are three control regions:

- $3\text{m/s} \leq V \leq 6.4\text{m/s}$. Minimum rotor speed. The rotor speed is regulated to the minimum value via a PI controller on the generator torque and a PI controller on the pitch angle. The pitch angle set-point is determined based on the optimal operational data calculated using HAWCStab2 during the stability analysis.
- $6.4\text{m/s} \leq V \leq 10.6\text{m/s}$. Optimal TSR. The rotor speed is regulated such that it operates at its optimal TSR via a PI controller on the generator torque.
- $10.6\text{m/s} \leq V \leq 25\text{m/s}$. Rated power. The rotor speed is regulated via a PI controller and the pitch angle is regulated via a PI controller. The regulation objectives are to keep the rotor speed at its rated value (7.6 RPM) and the generated power near the rated power. For floating application, the constant-power setting is traditionally replaced by constant generator torque.

The parameters for the DTU Basic Controller were determined using HAWCStab2's controller tuning feature. The assumed natural frequencies and damping for the partial and full load poles were [0.05 Hz, 0.7] and [0.06 Hz, 0.7], respectively. Quadratic gain scheduling was used with an assumption of constant power. The resulting controller parameters are given in Table 8. The definitions for all parameters and regions 1, 2 and 3 are consistent with the definitions in the DTU Basic Controller report.

Table 8: DTU Basic Control parameters for IEA 15 MW RWT

Parameter	Value
Quadratic torque controller coefficient for Region 1	0.264285E+08 Nm/(rad/s)^2
Proportional gain for torque controller in Region 2	0.164438E+09 Nm/(rad/s)
Integral gain for torque controller in Region 2	0.368998E+08 Nm/rad
Proportional gain for pitch controller in Region 3	0.177141E+01 rad/(rad/s)
Integral gain for pitch controller in Region 3	0.421192E+00 rad/rad
$K1$ term for quadratic gain scheduling	12.03781 deg
$K2$ term for quadratic gain scheduling	683.03643 deg^2

When inserting the controller parameters into the controller block in the HAWC2 input file, the parameters from the DTU 10MW were kept except for the following:

- Rated power, rated generator speed, minimum rotor speed and optimal TSR were updated.
- Maximum torque, maximum pitch rate and minimum pitch angle were updated to reflect the parameters in the `DISCON.in` file.
- The drivetrain frequency was updated to that from the IEA 15 MW (1.01Hz).
- All controller gains from the HAWCStab2 tuning procedure were updated.
- The maximum allowable tower acceleration was increased to 2.0 m/s^2 to allow for unpredicted vibrations.

The resulting system response to a step wind is shown in Fig. 14. The controller tuning results in a stable system, but there are undesirable vibrations near 11 and 12 m/s. Further work is needed to refine the controller parameters and remove these vibrations.

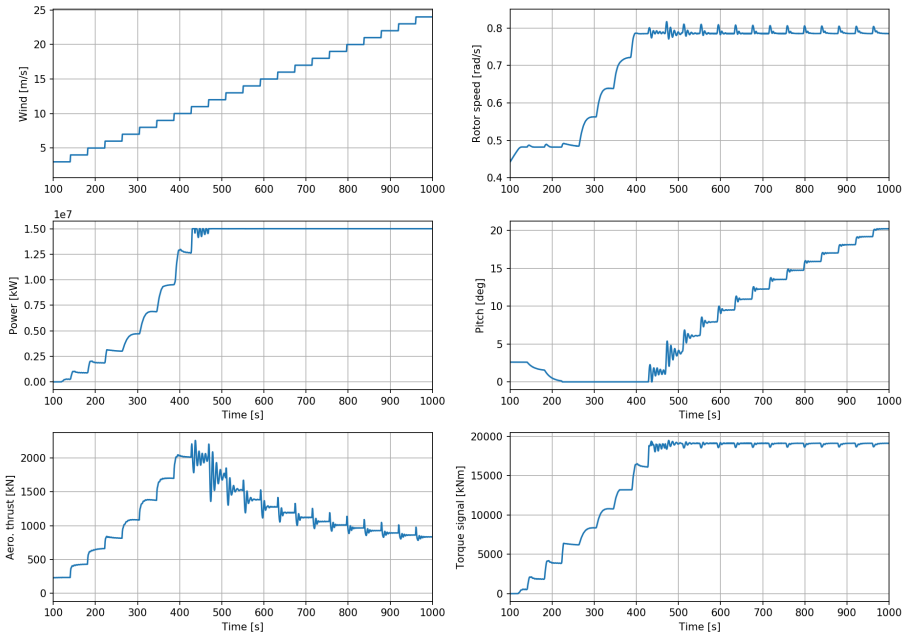

Figure 14: Turbine response to step wind

9 Addition of bend-twist coupling

Bend-twist coupling is a design feature that makes the blade twist when bended in the flap-wise direction. Hereby the angle of attach is reduced and the blade loads become smaller. It is thus a mechanism for passive load-alleviation which achieves some of the effects that classic pitch regulation yields for a stiff blade. The load reduction is of particular interest close to rated wind speed where the thrust is largest. It can be used to reduce the bending towards the tower and thus to achieve a better tower clearance,

An investigation was carried out exploring the effect of adding additional bend twist couplings into the blade through angling of the fibres in the spar caps. This was achieved by assuming a constant angular offset of the fibres starting from a spanwise location $r/R = 0.6$ (r=70m). Figure 15 shows the rotor AEP and maximum steady state flapwise moment under normal operation resulting from a range of spar cap fiber angles.

Additionally, Figure 16 shows the blade torsion and local thrust coefficient at 9 m/s across the computed range of material fiber angles. The baseline blade already torsions considerably under steady operation and is a fairly loads oriented design with low loading on the outer part of the blade, therefore we can observe that material coupling resulting in a nose-up torsional moment can increase the AEP by almost 1.5%. Bend-twist coupling resulting in additional unloading of the outer part of the blade (nose-down torsional deflection) is observed to result in up to approximately 10% reduction of the steady state flapwise moment for an 8 degree fiber orientation, but with a reduction in AEP of 2%.

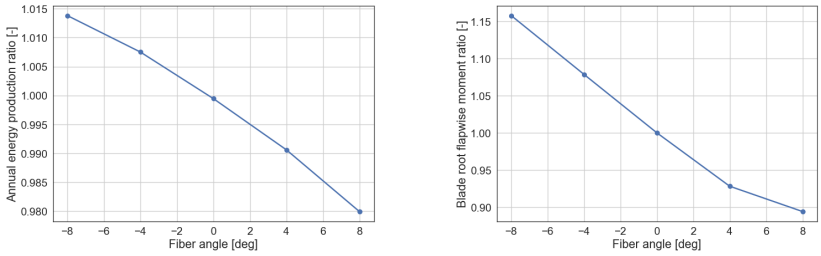

(a) Annual energy production ratio versus fiber angle.

(b) Blade root flapwise moment ratio versus fiber angle.

Figure 15: Influence of material fiber angle on steady state rotor AEP and blade root flapwise moment computed using HAWCStab2.

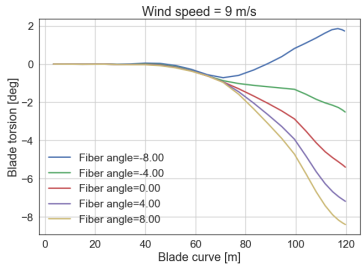

(a) Blade torsion vs blade-curve position at multiple fiber angles

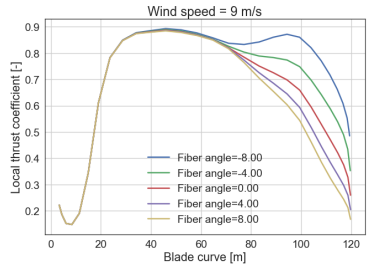

(b) Local thrust coefficient vs blade-curve position at multiple fiber angles

Figure 16: Influence of material fiber angle on steady state blade torsion and local thrust coefficient computed using HAWCStab2.

Figure 17 shows the rotor steady state performance of the material coupled blade with 8 degree fiber orientation compared to the baseline blade, where we as expected observe that the added torsional deflection results in a lower power production below rated power, as well as lower peak thrust and flapwise moments.

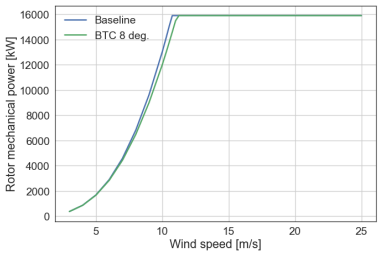

(a) Power curve

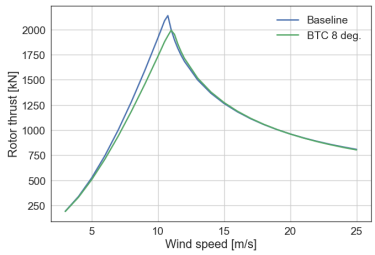

(b) Thrust curve

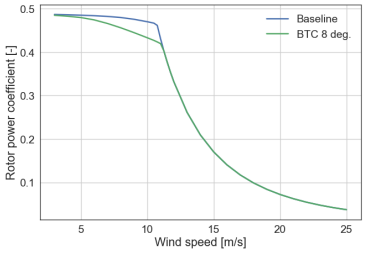

(c) Rotor global power coefficient

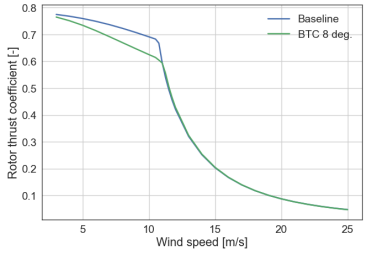

(d) Rotor global thrust coefficient

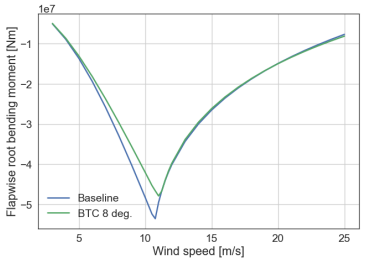

(e) Rotor global root flapwise moment

Figure 17: Rotor steady state aerodynamic performance of the bend-twist coupled blade with 8 degrees fiber orientation compared to the baseline blade computed with HAWCStab2.

10 Summary and outline of further work

The present report describes the HAWC2 implementation of the IEA 15 MW reference wind turbine as of end October 2019. Up to the official release of the turbine by the end of 2019, adjustments of the design are expected. These updates will be available at the Github site for the turbine.

Further work on the reference turbine include a monopile design at 30 m depth and a semi-submersible floater design by University of Maine.

Within COREWIND, the present HAWC2 model will provide the basis for the floater designs by COBRA and UPC. A first step in WP1 will be to provide also a FAST and a QuLAF model Pegalajar-Jurado, Borg, and Bredmose (2018) with the turbine on a generic floater.

For the floating application, adjustments of the tower design and controller are foreseen due to the coupling effects with the low-frequency modes of the floaters. The present investigation of bend-twist coupling shows that the coupling can be introduced to the design, but does not have a large effect for the present design, which already shows a decreasing local thrust towards the blade tip.

A Tower outer diameter and thickness

These are the original tables provided by NREL.

Table 9: Thickness of tower

Tower station	Wall thickness [m]
0.0000000000000000000e+00	4.92268900000000231e-02
1.5000000000000000000e+01	4.92268900000000231e-02
1.5000000000000000000e+01	4.58148199999999916e-02
3.0000000000000000000e+01	4.58148199999999916e-02
3.0000000000000000000e+01	4.30133700000000216e-02
4.5000000000000000000e+01	4.30133700000000216e-02
4.5000000000000000000e+01	4.12942199999999954e-02
6.0000000000000000000e+01	4.12942199999999954e-02
6.0000000000000000000e+01	3.93961800000000286e-02
7.5000000000000000000e+01	3.93961800000000286e-02
7.5000000000000000000e+01	3.67547199999999767e-02
9.0000000000000000000e+01	3.67547199999999767e-02
9.0000000000000000000e+01	3.34532700000000023e-02
1.0500000000000000000e+02	3.34532700000000023e-02
1.0500000000000000000e+02	2.98423100000000036e-02
1.2000000000000000000e+02	2.98423100000000036e-02
1.2000000000000000000e+02	2.62286400000000098e-02
1.3500000000000000000e+02	2.62286400000000098e-02
1.3500000000000000000e+02	3.06286300000000044e-02
1.4500000000000000000e+02	3.06286300000000044e-02

Table 10: Outer diameter of tower

Tower station	Outer diameter [m]
0.00000000000000000e+00	1.00000000000000000e+01
1.50000000000000000e+01	9.99993999999999161e+00
3.00000000000000000e+01	9.89329799999999703e+00
4.50000000000000000e+01	9.50122700000000089e+00
6.00000000000000000e+01	9.07381600000000770e+00
7.50000000000000000e+01	8.73373400000000108e+00
9.00000000000000000e+01	8.48125899999999659e+00
1.05000000000000000e+02	8.25469700000000173e+00
1.20000000000000000e+02	8.08723099999999170e+00
1.35000000000000000e+02	7.51252700000000399e+00
1.45000000000000000e+02	6.71754799999999853e+00

B Tower HAWC2 structural parameters

Here are the equations used to calculate the HAWC2 parameters for the tower.

B.1 Station, r [m]

- Summary: The distance along the tower from the base. For the onshore HAWC2 model, this is assumed to start at 0 m and end at 145.0 m. Thus, the tower model includes the transition piece, which extends from 0 to 15 m.
- Equations: None.

B.2 Mass per unit length, m [kg/m]

- Summary: Mass per unit length of the tower.
- Equations:

$$m = \rho A \tag{2}$$
$$= \rho \pi \left[(D/2)^2 - (D/2 - t)^2 \right], \tag{3}$$

where A is the cross-sectional area, D is the outer diameter and t is the wall thickness at a given station.

B.3 Center of mass, x_m [m]

- Summary: The x location of the center of mass. Because the tower is axisymmetric, this value is zero.
- Equations: $x_m = 0$.

B.4 Center of mass, y_m [m]

- Summary: The y location of the center of mass. Because the tower is axisymmetric, this value is zero.
- Equations: $y_m = 0$.

B.5 Radius of gyration, r_{ix} [m]

- Summary: Radius of gyration around principal bending axis x_e. We use the radius of gyration to calculate the mass moment of inertia for a cross-section, which we need for inertia calculations.
- Equations: For an isotropic circular tube,

$$r_{ix} = \sqrt{\frac{I_x}{A}}, \tag{4}$$

$$= \sqrt{\frac{\pi\left[(D/2)^4 - (D/2-t)^4\right]/4}{\pi\left[(D/2)^2 - (D/2-t)^2\right]}}, \tag{5}$$

$$= \sqrt{\frac{1}{4}\left[(D/2)^2 + (D/2-t)^2\right]}. \tag{6}$$

B.6 Radius of gyration, r_{iy} [m]

- Summary: Radius of gyration around principal bending axis y_e.
- Equations: Same as r_{ix} due to symmetry.

B.7 Shear center, x_s [m]

- Summary: The x coordinate of the shear center. Because the cross-section is symmetric about both x and y, the shear center is collocated with the elastic center (which is at the origin). **Andersen2008**
- Equations: $x_s = 0$

B.8 Shear center, y_s [m]

- Summary: The y coordinate of the shear center. Because the cross-section is symmetric about both x and y, the shear center is collocated with the elastic center (which is at the origin).
- Equations: $y_s = 0$

B.9 Young's modulus, E [Pa]

- Summary: The Young's modulus.
- Equations: Value in Table 3.

B.10 Shear modulus, G [Pa]

- Summary: Shear modulus.
- Equations: Value in Table 3.

B.11 Area moment of inertia, I_x [m^4]

- Summary: Area moment of inertia around principal bending axis x_e.
- Equations:

$$I_x = \int_A x^2 dxdy \tag{7}$$

$$= \frac{\pi}{4}\left[(D/2)^4 - (D/2-t)^4\right] \tag{8}$$

B.12 Area moment of inertia, I_y [m^4]

- Summary: Area moment of inertia around principal bending axis y_e.
- Equations:

$$I_y = \int_A y^2 dxdy \tag{9}$$

$$= \frac{\pi}{4}\left[(D/2)^4 - (D/2-t)^4\right] \tag{10}$$

B.13 Torsional stiffness constant, K [m^4/rad]

- Summary: Torsional stiffness constant calculated about the z axis at the shear center. Because we assume a circular section, this is equivalent to the polar moment of inertia.

- Equations:

$$K = \int_A r^2 dxdy, \tag{11}$$

$$= \frac{\pi}{2}\left[(D/2)^4 - (D/2-t)^4\right]. \tag{12}$$

B.14 Shear reduction factor, k_x [-]

- Summary: Shear factor, also called shear reduction factor, for shear in the x direction.
- Equations: Per **Hoogenboom2005**, we use the following shear factor:

$$k_x = \frac{1}{2} + \frac{3}{4}\frac{2t}{D}. \tag{13}$$

B.15 Shear reduction factor, k_y [-]

- Summary: Shear factor, also called shear reduction factor, for shear in the y direction.
- Equations: Per **Hoogenboom2005**, we use the following shear factor:

$$k_y = \frac{1}{2} + \frac{3}{4}\frac{2t}{D}. \tag{14}$$

B.16 Cross-sectional area, A [m^2]

- Summary: The area of the cross-section.
- Equations:

$$A = \int_A dxdy, \tag{15}$$

$$= \pi\left[(D/2)^2 - (D/2-t)^2\right]. \tag{16}$$

B.17 Structural pitch, θ_s [deg]

- Summary: This is the angle between x and the principle bending axis most parallel to x. Because the tower is axisymmetric, this is zero.
- Equations: $\theta_s = 0$).

B.18 Elastic center, x_e [m]

- Summary: The x location of the elastic center, which is the intersection point for the principle bending axes. Because the tower is axisymmetric about z, this is 0.
- Equations: $x_e = 0$.

B.19 Elastic center, y_e [m]

- Summary: The y location of the elastic center. Because the tower is axisymmetric about z, this is 0.
- Equations: $y_e = 0$.

References

Bak, C. et al. (2013). *Description of the DTU 10MW reference wind turbine*. Tech. rep. DTU Wind Energy Report I-0092. DTU Wind Energy.

Blasques, J. P. (2012). "User ' s Manual for BECAS A cross section analysis tool for anisotropic and inhomogeneous beam sections of arbitrary geometry e Pedro Blasques". In:

Blasques, J. P. and M. Stolpe (2012). "Multi-material topology optimization of laminated composite beam cross sections". In: *Composite Structures* 94(11), pp. 3278–3289. ISSN: 0263-8223. DOI: http://dx.doi.org/10.1016/j.compstruct.2012.05.002.

Bortolotti, P. et al. (2019). *IEA Wind TCP Task 37: Systems Engineering in Wind Energy - WP2.1 Reference Wind Turbines*. Tech. rep. International Energy Agency. DOI: 10.2172/1529216.

Desmond, C. et al. (2016). "Description of an 8 MW reference wind turbine". In: *Journal of Physics: Conference Series*. DOI: 10.1088/1742-6596/753/9/092013.

Hansen, M. H. and L. C. Henriksen (2013). *Basic DTU Wind Energy controller*. Tech. rep. DTU Wind Energy Report E-0018. DTU Wind Energy.

INNWIND.EU (2017). http://www.innwind.eu/publications/deliverable-reports.

Jonkman, J. et al. (2009). *Definition of a 5-MW Reference Wind Turbine for Offshore System Development*. Tech. rep. NREL/TP-500-38060. NREL.

Pegalajar-Jurado, A., M. Borg, and H. Bredmose (2018). "An efficient frequency-domain model for quick load analysis of floating offshore wind turbines". In: *Wind Energy Science* 3(2), pp. 693–712. ISSN: 2366-7443. DOI: 10.5194/wes-3-693-2018.

WindEurope (2019). *Offshore Wind in Europe. Key Trends and Statistics*. Tech. rep. WindEurope.

Zahle, F., C. Tibaldi, C. Pavese, et al. (2016). "Design of an Aeroelastically Tailored 10 MW Wind Turbine Rotor". In: *Journal of Physics: Conference Series* 753(6), p. 062008. URL: http://stacks.iop.org/1742-6596/753/i=6/a=062008.

Zahle, F., C. Tibaldi, D. R. Verelst, et al. (2015). "Aero-Elastic Optimization of a 10 MW Wind Turbine". In: *Proceedings - 33rd Wind Energy Symposium*. Vol. 1. American Institute of Aeronautics & Astronautics, pp. 201–223.